suggests that important roles are played by the relative orientation or distance of separation of the electron-transfer donor and acceptor in the electron-transfer act.

Acknowledgments are made to the National Science Foundation under Grant No. CHE-8503092 for support of this research.

Registry No. py-PTZ, 97170-93-9; PTZ, 92-84-2; 4-$ClCH_2$py, 10445-91-7; *fac*-[(bpy)Re$(CO)_3$(py-PTZ)](PF_6), 106818-73-9; (bpy)-Re$(CO)_3$(TFMS), 97170-94-0; [$(bpy)_2$RuCl(py-PTZ)](PF_6), 106735-80-2; $(bpy)_2RuCl_2$, 19542-80-4; [$(bpy)_2$Ru(CH_3CN)(py-PTZ)]$(PF_6)_2$, 106735-82-4; $(bpy)_2Ru(CO_3)$, 59460-48-9; *fac*-[(bpy)Re$(CO)_3$(4-Etpy)](PF_6), 84028-69-3; [(bpy)Re$(CO)_3$(py-PTZ$^{\bullet+}$)]$^{2+}$, 106735-83-5.

Contribution from the Chemistry Department,
The University of North Carolina, Chapel Hill, North Carolina 27514

Hydrogen Atom Transfer in the Oxidation of Hydrogen Peroxide by $[(bpy)_2(py)Ru^{IV}{=}O]^{2+}$ and by $[(bpy)_2(py)Ru^{III}{-}OH]^{2+}$

John Gilbert, Lee Roecker, and Thomas J. Meyer*

Received June 25, 1986

The oxidations of H_2O_2 and of HO_2^- by $[(bpy)_2(py)Ru^{IV}(O)]^{2+}$ and $[(bpy)_2(py)Ru^{III}(OH)]^{2+}$ have been studied in aqueous solution. Rate constants and activation parameters for the oxidation of H_2O_2 by $Ru^{IV}{=}O^{2+}$ are $k(25\ °C) = 1.74 \pm 0.18$, $\Delta H^{\ddagger} = 6.0 \pm 0.3$ kcal/mol, and $\Delta S^{\ddagger} = -37 \pm 3$ eu and by $Ru^{III}{-}OH^{2+}$ are $k(25\ °C) = (8.09 \pm 0.27) \times 10^{-2}$, $\Delta H^{\ddagger} = 12 \pm 2$ kcal/mol, and $\Delta S^{\ddagger} = -38 \pm 3$ eu. H_2O/D_2O kinetic isotope ratios are, for $Ru^{IV}{=}O^{2+}$, $(k_{H_2O}{}^{25°C}/k_{D_2O}{}^{25°C}) = 22.0 \pm 1.2$ and, for $Ru^{III}{-}OH^{2+}$, $(k_{H_2O}{}^{25°C}/k_{D_2O}{}^{25°C}) = 16.2 \pm 0.7$. From rapid-mixing experiments $[(bpy)_2(py)Ru^{III}(OH)]^{+}$ is the initial product of the oxidation of H_2O_2 by $Ru^{IV}{=}O^{2+}$ rather than $[(bpy)_2(py)Ru^{II}(OH_2)]^{2+}$, and it is proposed that oxidation of H_2O_2 by both $Ru^{IV}{=}O^{2+}$ and $Ru^{III}{-}OH^{2+}$ occurs by H atom (1e-1 H^+) transfer.

We report here the results of a kinetic and mechanistic investigation on the oxidation of hydrogen peroxide by the Ru(IV)-oxo complex *cis*-$[(bpy)_2(py)Ru(O)]^{2+}$. The basis for our interest in the reaction are as follows. (1) It has recently been discovered that related complexes oxidize water to oxygen, and since free or bound peroxide are possible intermediates, it was of value to discover the details of how H_2O_2 is oxidized further to O_2.[1] (2) For certain $Ru^{IV}{=}O^{2+}$-based organic oxidations, it has been proposed that the redox step involves a hydride transfer.[2-4] It would be invaluable to identify such a pathway

$$Ru^{IV}{=}O^{2+} + H_2O_2 \rightarrow Ru^{II}{-}OH^{+} + O_2 + H^{+}$$

$$Ru{-}OH^{+} + H^{+} \rightarrow RuOH_2{}^{2+}$$

or pathways

$$Ru^{IV}{=}O^{2+} + H_2O_2 \rightarrow Ru^{II}{-}OH_2{}^{2+} + O_2$$

in the oxidation of hydrogen peroxide. From the principle of microscopic reversibility the implications would be even more significant for O_2 reduction since it would suggest the possible existence of a concerted two-electron pathway in the reduction of O_2 to H_2O_2.

The iron porphyrin based enzymes catalase and peroxidase remove hydrogen peroxide from biological systems via two distinct mechanisms.[5] Catalase causes the decomposition of H_2O_2 by disproportionation into H_2O and O_2.[6] Peroxidase not only removes hydrogen peroxide but also takes advantage of its oxidizing equivalents to perform a variety of in vivo oxidations. The connection between these enzymes and $Ru^{IV}{=}O^{2+}$ may not be totally unreasonable in that a ferryl ($Fe^{IV}{=}O$) porphyrin group has been invoked as the active site in the enzymes.[7]

Although kinetic studies on reactions of inorganic compounds with hydrogen peroxide are numerous, many of them have focused either on complexes that contain coordination sites available for substitution by H_2O_2 (a step that can be rapid with respect to oxidation of H_2O_2) or on complexes that act strictly as outer-sphere oxidants.[8-17] The reaction of $[(bpy)_2(py)Ru(O)]^{2+}$ with hydrogen peroxide is particularly intriguing given the absence of a vacant or labile coordination site at the metal and the existence of several possible pathways for the mechanism that are more complex than simple outer-sphere electron transfer. As discussed elsewhere,[18] mechanistic evidence is available to suggest that oxo complexes of ruthenium are capable of acting as O atom donors or H atom or hydride acceptors, and all of these pathways are possibilities for the oxidation of H_2O_2. Part of this work has appeared as a preliminary communication.[19]

Experimental Section

Materials. House-distilled water was purified by distillation from alkaline permanganate. Reagent grade H_2O_2 (3%) was standardized by using $KMnO_4$ and primary standard grade As_2O_3.[20] More concentrated

(1) (a) Gersten, S. W.; Samuels, G. J.; Meyer, T. J. *J. Am. Chem. Soc.* **1982**, *104*, 4029. (b) Gilbert, J. A.; Eggleston, D. S.; Murphy, W. R., Jr.; Geselowitz, D. A.; Gersten, S. W.; Hodgson, D. J.; Meyer, T. J. *J. Am. Chem. Soc.* **1985**, *107*, 3855. (c) Honda, K.; Frank, A. J. *J. Chem. Soc., Chem. Commun.* **1984**, 635.
(2) Thompson, M. S.; Meyer, T. J. *J. Am. Chem. Soc.* **1982**, *104*, 5070.
(3) Thompson, M. S.; Meyer, T. J. *J. Am. Chem. Soc.* **1982**, *104*, 4106.
(4) Roecker, L.; Meyer, T. J. *J. Am. Chem. Soc.* **1986**, *108*, 4066.
(5) (a) Hewson, W. D.; Hager, L. P. In *The Porphyrins*; Dolphin, D., Ed.; Academic: New York, 1979; Vol. 7, p 295. (b) Duford, H. B.; Stillman, J. S. *Coord. Chem. Rev.* **1976**, *19*, 187.
(6) Hanson, L. K.; Chang, C. K.; Davis, M. S.; Fajer, J. *J. Am. Chem. Soc.* **1981**, *103*, 663.
(7) Dolphin, D. *Isr. J. Chem.* **1981**, *21*, 67.
(8) Galbacs, S. M.; Nagy, L.; Csanyi, L. J. *Polyhedron* **1982**, *1*, 175.
(9) Nagy, L.; Galbacs, Z. M.; Csanyi, L. J.; Horvath, L. *J. Chem. Soc., Dalton Trans.* **1982**, 859.
(10) Banas, B.; Mrozinski, J. *Proc. Conf. Coord. Chem.* **1980**, *8*, 11.
(11) Kozlov, Y. N.; Purmal, A. P.; Uskov, A. M. *Russ. J. Phys. Chem. (Engl. Transl.)* **1980**, *54*, 992.
(12) Sigel, H.; Flierl, C.; Griesser, R. *J. Am. Chem. Soc.* **1969**, *91*, 1061.
(13) Jarnigan, R. C.; Wang, J. H. *J. Am. Chem. Soc.* **1958**, *80*, 786.
(14) Held, A. M.; Halko, D. J.; Hurst, J. K. *J. Am. Chem. Soc.* **1978**, *100*, 5432.
(15) Heyward, M. P.; Wells, C. F. *J. Chem. Soc., Dalton Trans.* **1981**, 1863.
(16) Wells, C. F.; Fox, D. *J. Chem. Soc., Dalton Trans.* **1977**, 1498.
(17) Wells, C. F.; Husain, M. *J. Chem. Soc. A* **1970**, 1013.
(18) Meyer, T. J. *J. Electrochem. Soc.* **1984**, *131*, 221C.
(19) Gilbert, J. A.; Gersten, S. W.; Meyer, T. J. *J. Am. Chem. Soc.* **1982**, *104*, 6872.
(20) Vogel, A. I. *A. Textbook of Quantitative Inorganic Analysis*; Wiley: New York, 1961; p 295.

0020-1669/87/1326-1126$01.50/0

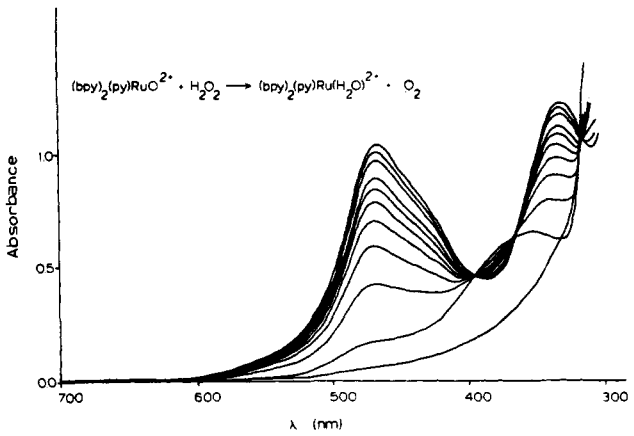

Figure 1. Repetitive UV–visible scans (5-min intervals) of the reaction of $[(bpy)_2(py)Ru(O)]^{2+}$ with H_2O_2 in excess at pH 2.3 showing the increases in absorbance associated with the initial appearance of $[(bpy)_2(py)Ru(OH)]^{2+}$ (λ_{max} = 365 nm) followed by the appearance of $[(bpy)_2(py)Ru(OH_2)]^{2+}$ (λ_{max} = 470). 397 and 372 nm are isosbestic points for $[(bpy)_2(py)Ru^{II}(OH_2)]^{2+}$ and $[(bpy)_2(py)Ru^{III}(OH)]^{2+}$.

solutions were prepared by dilution of 30% H_2O_2. All other materials were reagent grade and used without further purification.

For the kinetics experiments ionic strength was maintained at I = 0.1 M with the added buffer solution or added $LiClO_4$. pH was controlled by using $HClO_4$ with added $LiClO_4$ in acidic solution and in more basic solutions by using $H_2PO_4^-/HPO_4^{2-}$ buffers.

$[(bpy)_2(py)Ru^{II}(OH_2)](ClO_4)_2$ and $[(bpy)_2(py)Ru^{IV}(O)](ClO_4)_2$ were prepared by using literature procedures.[21,22] Solutions containing $[(bpy)_2(py)Ru^{III}(OH)]^{2+}$ were prepared by adding 1 equiv of Ce(IV) to a solution of $[(bpy)_2(py)Ru(OH_2)]^{2+}$ at pH 1.3.

$[(bpy)_2(py)Ru(^{18}O)](ClO_4)_2$. The ^{18}O labeled complex was prepared by using the procedure described by Moyer[21] with the following modification. A 24-mg sample of $[(bpy)_2(py)Ru(OH_2)](ClO_4)_2$ was added to 1.8 mL of $H_2{}^{18}O$ (97.5% ^{18}O, 0.5% ^{17}O, 2.0% ^{16}O; Isotec, Inc.). The solution was stirred and warmed to 30 °C overnight. A 10-μL aliquot of 70% $HClO_4$ was added followed by 2.05 equiv of $(NH_4)_2Ce(NO_3)_6$ resulting in immediate precipitation of 19 mg of the labeled product. IR analysis showed that ^{18}O labeling was quantitative within the limits of IR detection; only the $Ru{=}{}^{18}O$ stretch at 752 cm^{-1} could be observed. The $Ru{=}{}^{16}O$ stretch at 792 cm^{-1} was absent.

Instrumentation. Routine UV–visible spectra were recorded on either a Varian Model 634 spectrophotometer or a Bausch & Lomb Spectronic 2000 instrument. pH was measured with a Radiometer pHM62 pH meter. Mass spectral analyses were peformed at the Research Triangle Institute mass spectroscopy laboratory.

Labeling Study. In order to determine the origin of the oxygen evolved in the oxidation of H_2O_2 by $[(bpy)_2(py)Ru(O)]^{2+}$, 15 mg of the ^{18}O labeled Ru(IV) complex were placed in a 25-mL round-bottom reaction flask, which was connected to a 100-mL gas bulb. The system was purged with argon, and the gas bulb was evacuated. A 5-mL aliquot of a solution containing 0.1 M CF_3SO_3H and 2 equiv of H_2O_2 was injected into the reaction flask via a syringe through a septum. When the reaction was complete, the evolved gas was transferred to the gas bulb and the gas bulb was removed for mass spectral analysis.

Kinetics. Kinetics of reactions with half-lives of less than 5 min were followed by sample mixing. Faster reactions were followed by using an Aminco-Morrow stopped-flow mixing chamber attached to a Beckman Model DU monochromator, details of which are described elsewhere.[23] Absorbance vs. time traces were analyzed as ln $(A - A_t)$ vs. time by an automatic data handling program.

Rate data for the disappearance of Ru(IV) were collected by following the absorbance increase at 397 nm. This wavelength is an isosbestic point for $[(bpy)_2(py)Ru^{III}(OH)]^{2+}$ and $[(bpy)_2(py)Ru^{II}(OH_2)]^{2+}$, and the disappearance of Ru(IV) can be followed without any contribution from the subsequent reduction of Ru(III) to Ru(II).

Rate data for the disappearance of Ru(III) were collected by following the formation of Ru(II) at 470 nm. Plots of ln $(A - A_t)$ vs. time for this reaction were nonlinear because of contributions to the oxidation of H_2O_2, by initial disproportionation to Ru(IV), 2Ru(III) → Ru(IV) + Ru(II), followed by oxidation of H_2O_2 by Ru(IV).[2] Linearity could be significantly improved by adding approximately 1 equiv of $[(bpy)_2(py)Ru^{II}(OH_2)]^{2+}$ to suppress the disproportionation.

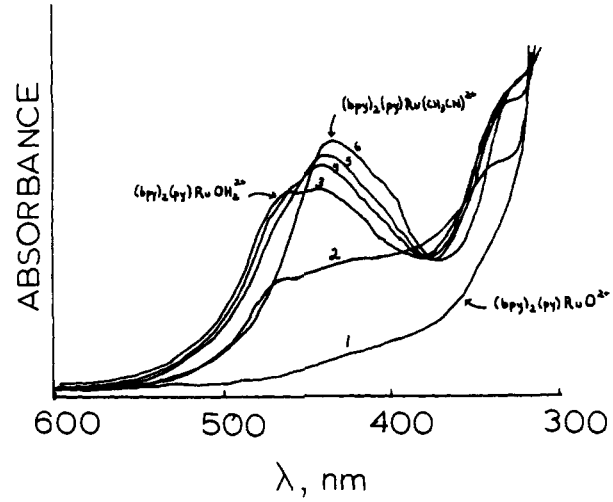

Figure 2. Repetitive UV–visible scans of the reaction between $[(bpy)_2(py)Ru(O)]^{2+}$ and a few drops of 30% H_2O_2 in acetonitrile at 8-min intervals.

Results

Stoichiometry. The addition of H_2O_2 to aqueous solutions of $[(bpy)(py)Ru^{IV}(O)]^{2+}$ results in spectral changes consistent with the reduction of Ru(IV) to $[(bpy)_2(py)Ru^{II}(OH_2)]^{2+}$ (Figure 1) through the intermediacy of $[(bpy)_2(py)Ru^{III}(OH)]^{2+}$. The results of a spectrophotometric titration showed that the conversion of Ru(IV) to Ru(II) is complete after the addition of 1 mol of H_2O_2/mol of Ru(IV). GC analysis of the gas evolved from the reaction confirmed that the reaction product is O_2 in the expected amount and that the stoichiometry of the net reaction is

$$[(bpy)_2(py)Ru^{IV}(O)]^{2+} + H_2O_2 \rightarrow [(bpy)_2(py)Ru^{II}(OH_2)]^{2+} + O_2 \quad (1)$$

The appearance of $[(bpy)_2(py)Ru^{III}(OH)]^{2+}$ as an intermediate suggests that the overall reaction occurs in a stepwise manner

$$2[(bpy)_2(py)Ru^{IV}(O)]^{2+} + H_2O_2 \rightarrow 2[(bpy)_2(py)Ru^{III}(OH)]^{2+} + O_2 \quad (2)$$

$$2[(bpy)_2(py)Ru^{III}(OH)]^{2+} + H_2O_2 \rightarrow 2[(bpy)_2(py)Ru^{II}(OH_2)]^{2+} + O_2 \quad (3)$$

The results of a repetitive scan experiment in acetonitrile with a few drops of added 30% H_2O_2 are shown in Figure 2. Note that the Ru(II) product of the reaction initially appears as $[(bpy)_2(py)Ru^{II}(OH_2)]^{2+}$, which undergoes subsequent solvation to yield $[(bpy)_2(py)Ru^{II}(CH_3CN)]^{2+}$. The mechanistic implications of this observation are discussed in a later section. The halftime for solvation by CH_3CN is ~8 min at 25 °C.

Kinetic Studies. Plots of ln ΔA vs. t ($\Delta A = (A_\infty - A_t)$) under pseudo-first-order conditions in H_2O_2 were linear for at least 2–3 half-times. Because 397 nm is an isosbestic point for $[(bpy)_2(py)Ru^{II}(OH_2)]^{2+}$ and $[(bpy)_2(py)Ru^{III}(OH)]^{2+}$, values taken at 397 nm allowed the first, Ru(IV) stage in the oxidation of H_2O_2 (reaction 2) to be studied without interferences from the second, Ru(III) stage.

The first-order dependence of the observed rate constant on $[H_2O_2]$ is shown in Figure 3, and second-order rate constants calculated from the slopes of $[H_2O_2]$ vs. k_{obsd} plots at different pH values are listed in Table I. In Table II are listed data for the oxidation of H_2O_2 by $[(bpy)_2(py)Ru(OH)]^{2+}$ in the presence of added $[(bpy)_2(py)Ru(OH_2)]^{2+}$ to suppress the disproportionation-based pathway. Typical absorbance–time and ln $(A_\infty - A_t)$ vs. t plots are shown in Figure 1S (supplementary material).

(21) Moyer, B. A. Ph.D. Dissertation, The University of North Carolina, Chapel Hill, NC, 1980.
(22) Moyer, B. A.; Meyer, T. J. *Inorg. Chem.* **1981**, *20*, 436.
(23) Cramer, J. L. Ph.D. Dissertation, University of North Carolina, Chapel Hill, NC, 1975, pp 191–216.

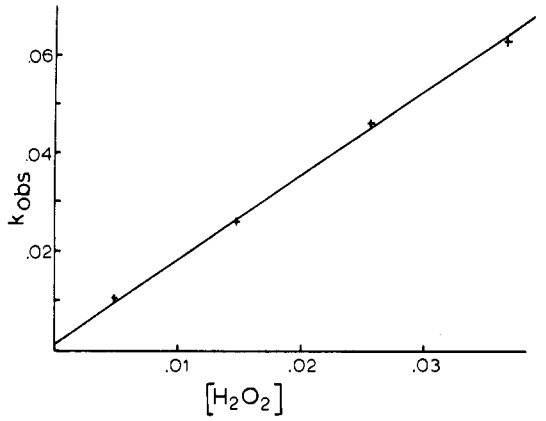

Figure 3. Plot of k_{obsd} vs. $[H_2O_2]$ for the reaction between $[(bpy)_2(py)Ru(O)]^{2+}$ and H_2O_2 at pH 2.3, 25.0 ± 0.1 °C, and I = 0.1 M.

Table I. Kinetics Data for the Oxidation of H_2O_2 by $[(bpy)_2(py)Ru^{IV}(O)]^{2+}$ [a] at 25.0 ± 0.1 °C, I = 0.1 M

pH[a]	$[H_2O_2]$, M	10^5[Ru(IV)], M	k_{obsd}, s^{-1}	k',[b,c] M^{-1} s^{-1}
2.37	8.50×10^{-3}	4.45	0.0198	
			0.0194	
			0.0185	
			0.0191	
	2.12×10^{-2}		0.0454	
			0.0468	2.10 ± 0.07
			0.0445	
	3.40×10^{-2}		0.0706	
			0.0707	
			0.0760	
			0.0707	
7.92	6.37×10^{-4}	4.07	0.0137	
			0.0143	
	2.12×10^{-3}		0.0256	
			0.0275	12.7 ± 1.3
			0.0309	
	3.83×10^{-3}		0.0530	
			0.0490	
			0.0460	
9.11	6.37×10^{-4}	4.37	0.114	
			0.104	
			0.114	
	2.12×10^{-3}		0.251	83.6 ± 7.3
			0.250	
	3.83×10^{-3}		0.380	
			0.371	
9.75	8.50×10^{-3}	6.60	2.79	
			2.72	
			2.85	
			2.86	
	2.12×10^{-2}		5.83	
			5.91	190 ± 26
			6.10	
	3.40×10^{-2}		7.66	
			7.14	
			7.73	
			8.07	
10.08	6.37×10^{-4}	4.15	0.506	
			0.492	
			0.523	
	2.12×10^{-3}		1.63	
			1.68	684 ± 63
			1.77	
	3.82×10^{-3}		2.56	
			2.54	

[a] Ionic strength and pH maintained with $LiClO_4/HClO_4$ or $HPO_4^{2-}/H_2PO_4^-$ buffers; pH ±0.05. [b] Error limits of rate constants cited are the 95% confidence limits. [c] $k' = k_{obsd}/[H_2O_2]$ as evaluated from the slopes of plots of k_{obsd} vs. $[H_2O_2]$.

Rate constants for both the Ru(IV) and Ru(III) reactions were measured as a function of temperature at pH 2.3 and 9.75. The results appear in Table 1S (supplementary material). The enthalpies and entropies of activation shown in Table III were obtained from plots of ln (k/T) vs. $1/T$ according to the reaction rate theory expression

$$\ln\left(\frac{k}{T}\right) = \frac{-\Delta H^{\ddagger}}{RT} + \frac{\Delta S^{\ddagger}}{R} + \frac{k_B}{h} \qquad (4)$$

by using the data in Figures 2S and 3S (supplementary material).

Table II. Rate Constants for the Oxidation of H_2O_2 by $[(bpy)_2(py)Ru^{III}(OH)]^{2+}$ [a] at 25.0 ± 0.1 °C, I = 0.1 M[a]

pH[a]	$10^2[H_2O_2]$, M	10^5[Ru(III)],[b] M	k_{obsd}, s^{-1}	k',[c,d] M^{-1} s^{-1}
2.30	5.15	5.5	2.78×10^{-3}	
			2.85×10^{-3}	5.4×10^{-2}
			2.77×10^{-3}	
9.75	2.09	2.7	9.83×10^{-2}	
			9.75×10^{-2}	
			9.89×10^{-2}	
			9.88×10^{-2}	
			9.35×10^{-2}	
	4.19		1.86×10^{-1}	
			1.79×10^{-1}	
			1.83×10^{-1}	
			1.80×10^{-1}	3.68 ± 0.08
			1.82×10^{-1}	
	8.45		3.36×10^{-1}	
			3.31×10^{-1}	
			3.32×10^{-1}	
			3.35×10^{-1}	

[a] Ionic strength and pH maintained by added $LiClO_4/HClO_4$ or $HPO_4^{2-}/H_2PO_4^-$ buffers; pH ±0.05. [b] In the presence of equimolar $[(bpy)_2(py)Ru^{II}(OH_2)]^{2+}$ in order to suppress contributions to the oxidation from initial disproportionation of Ru^{III}—OH^{2+} followed by oxidation by Ru^{IV}=O^{2+}. See text. [c] Error limits of rate constants are the 95% confidence limits. [d] $k' = k_{obsd}/[H_2O_2]$.

By using the data in Figures 2S and 3S (supplementary material).

Rate constant data obtained in D_2O at pH 2.3 and pH 9.75 are listed in Table IV, and for comparison rate constants measured in H_2O are included under the same conditions. The temperature dependence of the Ru(IV) reaction in D_2O at pH 2.3 was measured as a function of temperature and the $\Delta H^{\ddagger}$ and $\Delta S^{\ddagger}$ values are shown in Table III. The plot of ln (k/T) vs. $1/T$ for the reaction is shown in Figure 4S (supplementary material).

^{18}O Labeling Study. Mass spectral analysis of the gas evolved from the reaction between $[(bpy)_2(py)Ru^{IV}(^{18}O)]^{2+}$ (5×10^{-4} M) and H_2O_2 (10^{-3} M) showed ^{16}O–^{16}O to be the gaseous product with no evidence for ^{16}O–^{18}O.

Rapid-Mixing Experiments To Distinguish between 1- and 2-Electron Pathways. Although the oxidation of H_2O_2 by $[(bpy)_2(py)Ru^{III}(OH)]^{2+}$ must occur by an initial 1-electron step, the initial step in oxidation by $[(bpy)_2(py)Ru^{IV}(O)]^{2+}$ could involve either 1 or 2 electrons. It is possible to make a distinction between the two by rapid-mixing experiments. In the case of 1-electron transfer, $[(bpy)_2(py)Ru^{III}(OH)]^{2+}$ would be the sole initial product via

$$[(bpy)_2(py)Ru^{IV}{=}O]^{2+} + H_2O_2 \rightarrow [(bpy)_2(py)Ru^{III}{-}OH]^{2+} + HO_2$$

only if it appears in the first step and if HO_2 is selectively scavenged by Ru(IV) in the second step

$$[(bpy)_2(py)Ru^{IV}{=}O]^{2+} + HO_2 \rightarrow [(bpy)_2(py)Ru^{III}{-}OH]^{2+} + O_2$$

For 2-electron transfer the initial product would be Ru(II)

$$[(bpy)_2(py)Ru^{IV}{=}O]^{2+} + H_2O_2 \rightarrow [(bpy)_2(py)Ru^{II}{-}OH_2]^{2+} + O_2$$

However, there are two complications associated with the interpretation of simple mixing experiments. Once formed in the presence of Ru(IV), Ru(II) undergoes rapid comproportionation[24,25]

$$[(bpy)_2(py)Ru^{II}{-}OH_2]^{2+} + [(bpy)_2(py)Ru^{IV}{=}O]^{2+} \rightarrow 2[(bpy)_2(py)Ru^{III}{-}OH]^{2+}$$

$$k(I = 0.1\ M,\ 25\ °C) = 2.1 \times 10^5\ M^{-1}\ s^{-1}$$

Table III. Activation Parameters and k_{H_2O}/k_{D_2O} for the Oxidation of H_2O_2, I = 0.1 M[a]

reaction	pH or pD	medium	k(25 °C), M^{-1} s^{-1}	$\Delta H^{\ddagger}$, kcal/mol	$\Delta S^{\ddagger}$, eu	k_{H_2O}/k_{D_2O} (25 °C)
Ru(IV) + H_2O_2	2.3	H_2O	1.74 ± 0.18[b]	6.0 ± 0.3	−37 ± 3	22.0 ± 1.2
		D_2O	(8.09 ± 0.27) × 10^{-2}[b]	9.2 ± 1.2	−35 ± 4	
Ru(IV) + HO_2^-	9.7	H_2O	(2.64 ± 0.17) × 10^4[c]	3.5 ± 0.4	−27 ± 3	8.0 ± 2.9
Ru(III) + H_2O_2	2.3	H_2O	(5.44 ± 0.12) × 10^{-2}[d]	12 ± 2	−23 ± 5	16.2 ± 0.7
Ru(III) + HO_2^-	9.7	H_2O	(2.87 ± 0.20) × 10^2[e]	1.4 ± 0.3	−38 ± 3	

[a] Using $HClO_4/LiClO_4$ or $HPO_4^{2-}/H_2PO_4^-$ buffers. [b] $k_{1,IV}$ in eq 5 of the text. [c] $k_{2,IV}$ in eq 5a. [d] $k_{1,III}$. [e] $k_{2,III}$ in eq 5b.

Table IV. Rate Constant Data in H_2O and D_2O, I = 0.1 M at 25.0 ± 0.1 °C

reaction	pH or pD[a]	$[H_2O_2]$, M	[Ru], M	k_{obsd}, s^{-1}	k',[b] M^{-1} s^{-1}
Ru(IV) + H_2O_2 in D_2O	2.3	0.0364	6.1×10^{-4}	2.48×10^{-3}	
				2.46×10^{-3}	
		0.0256		1.61×10^{-3}	
		0.0205		1.17×10^{-3}	(7.92 ± 0.27) × 10^{-2}
		0.0147		7.72×10^{-4}	
Ru(IV) + H_2O_2 in H_2O	2.3	0.0364	5.8×10^{-4}	6.34×10^{-2}	
		0.0256		4.64×10^{-2}	1.74 ± 0.18
		0.0147		2.60×10^{-2}	
		0.00590		1.06×10^{-2}	
		(k_{H_2O}/k_{D_2O}) = 21.6 ± 1.2[b]			
reaction	pH[a]	$[H_2O_2]$, M	[Ru], M	k_{obsd}, s^{-1}	k',[b] M^{-1} s^{-1}
Ru(IV) + H_2O_2 in D_2O	9.75	0.000637	4.1×10^{-5}	2.16×10^{-2}	
				2.22×10^{-2}	
		0.00191		5.28×10^{-2}	
				5.29×10^{-2}	22.6 ± 2.9
		0.00382		1.01×10^{-1}	
				8.9×10^{-2}	
				9.3×10^{-2}	
		(k_{H_2O}/k_{D_2O}) = 8.04 ± 2.83[b]			
Ru(III) + H_2O_2 in H_2O	2.3	0.0515	5.5×10^{-3}	2.78×10^{-3}	
				2.89×10^{-3}	(5.44 ± 0.08) × 10^{-2}
				2.77×10^{-3}	
Ru(III) + H_2O_2 in D_2O	2.3	0.0515	5.7×10^{-5}	1.83×10^{-4}	
				1.71×10^{-4}	(3.36 ± 0.17) × 10^{-3}
				1.66×10^{-4}	
		(k_{H_2O}/k_{D_2O}) = 16.2 ± 0.67[b]			

[a] pH ±0.05 using $HClO_4/LiClO_4$ or $HPO_4^{2-}/H_2PO_4^-$ buffers. [b] Error limits of rate constants are the 95% confidence limits; error limits of k_{H_2O}/k_{D_2O} values are the standard deviation.

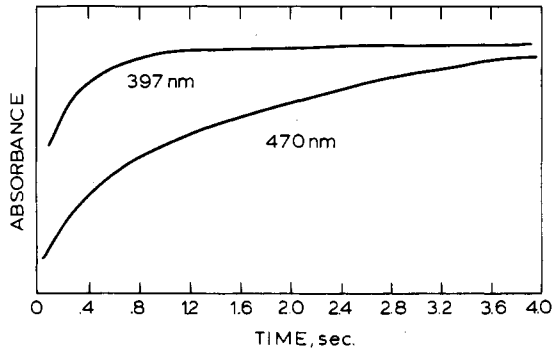

Figure 4. Stopped-flow traces at 397 and 470 nm following mixing of solutions containing $[(bpy)_2(py)Ru(O)]^{2+}$ and H_2O_2 at 25 °C. After the solutions were mixed, [Ru(IV)] = 8.86 × 10^{-6} M, $[H_2O_2]$ = 1.93 M, I = 0.05 M, and $[H^+]$ = 0.05 M. The traces show the rapid appearance of Ru(III) at 397 nm followed by the slower appearance of Ru(II) at 470 nm.

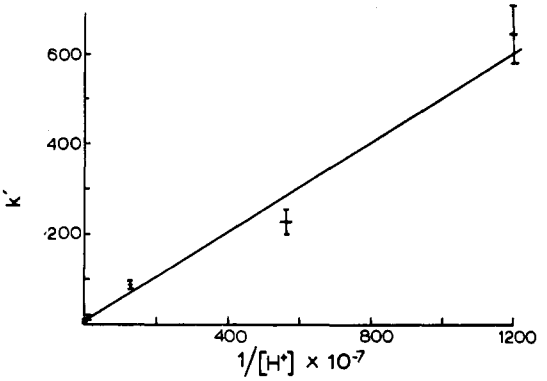

Figure 5. Plot of k_{obsd} vs. $[H^+]^{-1}$ for the oxidation of H_2O_2 by $[(bpy)_2(py)Ru(O)]^{2+}$ at 25.0 ± 0.1 °C, I = 0.1 M.

and in order to avoid comproportionation as a source of Ru(III), mixing experiments must be carried out at high H_2O_2 concentrations where $t_{1/2}(H_2O_2$ oxidation) < $t_{1/2}$ (comproportionation). The second complication is that once formed, Ru(III) also oxidizes H_2O_2 at a reasonably rapid rate. As a consequence, the mixing experiment must be carried out at high $[H_2O_2]$ in a stopped-flow spectrometer on a time scale that is short compared to the time scale for the oxidation of H_2O_2 by Ru(III).

The results of one such experiment are shown in Figure 4. The rapid initial appearance of Ru(III) is shown by the increase in absorbance at the Ru(II)–Ru(III) isosbestic point at 397 nm. Under these conditions $t_{1/2}(H_2O_2$ oxidation) is ~6–7 times shorter than the half-time for comproportionation. In Figure 4 is also shown the slower appearance of Ru(II) at 470 nm, which arises from oxidation of H_2O_2 by Ru(III). From the experiment Ru(III) is the dominant initial product in the oxidation of H_2O_2 by $Ru^{IV}{=}O^{2+}$, and the reaction occurs by a 1-equiv pathway.

The experiment in Figure 4 was carried out in acidic solution where the net reaction is dominated by the Ru(IV) oxidation of H_2O_2. At pH 9.0 where oxidation of HO_2 dominates the reaction (see below) a stopped-flow experiment at $[H_2O_2]$ = 0.35 M and

(24) Binstead, R. A.; Moyer, B. A.; Samuels, G. J.; Meyer, T. J. *J. Am. Chem. Soc.* **1981**, *103*, 2897.
(25) Binstead, R. A.; Meyer, T. J. *J. Am. Chem. Soc.*, in press.

[Ru(IV)] = 1.4×10^{-4} M gave the same result shown in Figure 4 but on a shorter time scale consistent with the more rapid oxidation at pH 9.0.[26]

Discussion

Rate Laws. The pH dependence of k_{obsd} for the oxidation of H_2O_2 by $[(bpy)_2(py)Ru(O)]^{2+}$ is consistent with the rate law in eq 5, which is shown graphically by the variations of k_{obsd} with

$$-d[Ru(IV)]/dt = [H_2O_2][Ru(IV)](k_{1,IV} + k'_{2,IV}[H^+]^{-1}) \quad (5)$$

$[H^+]^{-1}$ in Figure 5. The relatively simple form of the rate law arises because $K_{a,1}(25\ °C, I = 0.1\ M) = 2.28 \times 10^{-12}$ for H_2O_2,[27] and H_2O_2 is by far the dominant form of hydrogen peroxide even at the highest pH value (9.75) used in our kinetic studies.

$$k_{obsd} = k_{1,IV} + k'_{2,IV}[H^+]^{-1}$$

Assuming that the path inverse in $[H^+]$ involves oxidation of HO_2^- by $Ru^{IV}{=}O^{2+}$, the inverse acid term in the rate law can be written as

$$k_{2,IV}[Ru(IV)][HO_2^-] = \frac{k'_{2,IV}[H_2O_2]}{K_{a,1}[H^+]}[Ru(IV)]$$

and $k_{2,IV}$ is related to $K_{a,1}$ for H_2O_2 and the experimentally observed rate constant $k'_{2,IV}$ by

$$k_{2,IV} = k'_{2,IV}/K_{a,1} \quad (5a)$$

Using $K_{a,1}(25\ °C, I = 0.1\ M) = 2.28 \times 10^{-12}$ and $k'_{2,IV} = (6.03 \pm 0.38) \times 10^{-8}\ s^{-1}$ from the slope in Figure 5 gives $k_{2,IV}(I = 0.1\ M, 25\ °C) = (2.64 \pm 0.17) \times 10^4\ M^{-1}\ s^{-1}$ as shown in Table III.

In acidic solution, at pH 2.3, the oxidation of H_2O_2 is carried essentially completely by the $Ru{=}O^{2+} + H_2O_2$ path, and in basic solution, at pH 9.75, the reaction is carried by the $Ru{=}O^{2+} + HO_2^-$ path. pH 2.3 and 9.75 were the conditions used to establish isotope effects and temperature dependences for the acid-dependent and acid-independent pathways.

The kinetics of oxidation of H_2O_2 by $[(bpy)_2(py)Ru^{III}(OH)]^{2+}$ were also investigated at pH 2.3 and 9.75 (Table II). In competition with the direct reaction between $Ru^{III}OH^{2+}$ and H_2O_2 ($k_{2,III}$) is a pathway involving initial disproportionation, $2Ru^{III}{-}OH^{2+} \rightarrow Ru^{IV}{=}O^{2+} + Ru^{II}{-}OH_2^{2+}$, followed by oxidation of H_2O_2 by $Ru^{IV}{=}O^{2+}$.[2] The data summarized in Table II were obtained in the presence of added $[(bpy)_2(py)Ru(OH_2)]^{2+}$ to suppress the pathway involving initial disproportionation. Assuming that the oxidation of H_2O_2 by Ru(III) at pH 9.75 occurs dominantly via HO_2^-, the rate constant $k_{2,III}$ in the rate term

$$k_{2,III}[Ru(III)][HO_2^-] = \frac{k'_{2,III}[H_2O_2]}{K_{a,1}[H^+]}[Ru(III)] \quad (5b)$$

is $k_{2,III}(25\ °C, I = 0.1\ M) = (2.87 \pm 0.20) \times 10^2\ M^{-1}\ s^{-1}$.

Mechanistic Considerations. In addition to the rate laws, a number of results bear directly on the question of mechanism. The most striking is the observation of significant k_{H_2O}/k_{D_2O} kinetic isotope effects (Table III) for the acid-independent paths for oxidation by $Ru^{IV}O^{2+}$ or $Ru^{III}{-}OH^{2+}$. The experiment does not factor the isotope effect between solvent, H_2O/D_2O, and substrate, H_2O_2/D_2O_2. However, k_{H_2O}/k_{D_2O} kinetic isotope effects in, for example, outer-sphere electron-transfer reactions are normally quite small,[28] suggesting that the majority of the effect arises from the exchange of D for H in H_2O_2. Sizable C–H-based H/D kinetic isotope effects have been reported for oxidations involving $Ru^{IV}{=}O^{2+}$ and alcohols[3,29] or formate ion,[4] and large O–H-based effects have been observed in the oxidations of hydroquinone[30] or $[(bpy)_2(py)Ru(OH_2)]^{2+}$.[24,25] The results of the rapid-mixing experiments show that the oxidations of either H_2O_2 or HO_2^- by $Ru^{IV}{=}O^{2+}$ occur largely by 1-electron steps to give $[(bpy)_2(py)Ru^{III}(OH)]^{2+}$ as the initial product.

The appearance of $^{16}O{-}^{16}O$ as the product of the reaction between $H{-}^{16}O^{16}OH$ and $[(bpy)_2(py)Ru^{IV}(^{18}O)]^{2+}$ shows that O atom transfer from $Ru^{IV}{=}O^{2+}$ to H_2O_2 does not occur. Earlier ^{18}O labeling studies based on a series of oxidants including catalase have also shown that the O atoms in H_2O_2 are retained in the O_2 product.[13]

The combination of rate law, k_{H_2O}/k_{D_2O} kinetic isotope effect, and initial product studies show that the oxidation of H_2O_2 by $Ru^{IV}{=}O^{2+}$ occurs by a 1-electron pathway that involves the $H{-}O_2H$ bond in an intimate manner. For both $Ru^{IV}{=}O^{2+}$ and $Ru^{III}{-}OH^{2+}$, the available evidence suggests that following preassociation between reactants, the key redox event is the simultaneous transfer of an electron and proton (H atom transfer) from H_2O_2 to the oxidant whether it be $Ru^{IV}{=}O^{2+}$ (b is 2,2′-bipyridine)

$$[b_2(py)Ru^{IV}{=}O]^{2+} + H_2O_2 \underset{K'_{IV,H_2O_2}}{\rightleftharpoons} [b_2(py)Ru^{IV}{=}O]^{2+},H_2O_2 \quad (6)$$

$$[b_2(py)Ru^{IV}{=}O]^{2+},H_2O_2 \xrightarrow[k_{IV,H_2O_2}]{} [b_2(py)Ru^{III}{-}OH]^{2+},HO_2 \quad (7)$$

or $Ru^{III}{-}OH^{2+}$

$$[b_2(py)Ru^{III}{-}OH]^{2+} + H_2O_2 \underset{K'_{III,H_2O_2}}{\rightleftharpoons} [b_2(py)Ru^{III}{-}OH]^{2+},H_2O_2 \quad (8)$$

$$[b_2(py)Ru^{III}{-}OH]^{2+},H_2O_2 \xrightarrow[k_{III,H_2O_2}]{} [b_2(py)Ru^{II}{-}OH_2]^{2+},HO_2 \quad (9)$$

From the initial appearance of $Ru^{III}{-}OH^{2+}$ rather than $Ru^{II}{-}OH_2^{2+}$ in the rapid-mixing experiments, two additional conclusions can be reached concerning the oxidation by $Ru^{IV}{=}O^{2+}$. Past the H atom transfer step, further oxidation of HO_2 by $Ru^{III}{-}OH^{2+}$ is slow compared to separation of the reactants from the surrounding solvent cage, $k_{-D} > k_{redox}$

$$[b_2(py)Ru^{III}{-}OH]^{2+},HO_2 \begin{cases} \xrightarrow{k_{-D}} [b_2(py)Ru^{III}{-}OH]^{2+} + HO_2 \\ \xrightarrow{k_{redox}} [b_2(py)Ru^{II}{-}OH_2]^{2+},O_2 \end{cases}$$

Once formed in solution, the perhydroxyl radical must be oxidized more rapidly by $Ru^{IV}{=}O^{2+}$

$$[b_2(py)Ru^{IV}{=}O]^{2+} + HO_2 \rightarrow [b_2(py)Ru^{III}{-}OH]^{2+} + O_2$$

than by $Ru^{III}{-}OH^{2+}$

$$[b_2(py)Ru^{III}{-}OH]^{2+} + HO_2 \rightarrow [b_2(py)Ru^{II}{-}OH_2]^{2+} + O_2$$

The relatively sizable k_{H_2O}/k_{D_2O} kinetic isotope effect for the oxidation of HO_2^- by $Ru^{IV}{=}O^{2+}$ may be deceiving mechanistically. The experimentally observed rate constant is the product of the rate constant for the redox step and the first acid dissociation constant for H_2O_2, $k'_{2,IV} = k_{2,IV}K_{a,1}$. Although $K_{a,1}$ for D_2O_2 appears not to have been measured, $K_{a,1}(H_2O)/K_{a,1}(D_2O) = 7.28$.[31] If a similar isotope effect exists for H_2O_2, only a small H_2O/D_2O kinetic isotope effect exists for the redox step ($k_{2,IV}$) and the mechanism may involve outer-sphere electron transfer

(26) Gilbert, J. A. Ph.D. Dissertation, University of North Carolina, Chapel Hill, NC, 1983.
(27) Evans, M. G.; Uri, N. *Trans. Faraday Soc.* **1949**, *45*, 224.
(28) (a) Guarr, T.; Buhks, E.; McLendon, G. *J. Am. Chem. Soc.* **1983**, *105*, 3763. (b) Weaver, M. J.; Tyrra, P. D.; Nettles, S. M. *J. Electroanal. Chem. Interfacial Electrochem.* **1980**, *114*, 53.
(29) Roecker, L.; Meyer, T. J. *J. Am. Chem. Soc.* **1987**, *109*, 746.
(30) Roecker, L. Ph.D. Dissertation, The University of North Carolina, Chapel Hill, NC, 1985.
(31) Gold, V.; Lowe, B. M. *J. Chem. Soc. A* **1967**, 936.

$$H_2O_2 \underset{K_{a1}}{\rightleftharpoons} HO_2^- + H^+$$

$$[b_2(py)Ru^{IV}{=}O]^{2+} + HO_2^- \underset{K_{IV,HO_2^-}}{\rightleftharpoons} [b_2(py)Ru^{IV}{=}O]^{2+},HO_2^- \quad (10)$$

$$[b_2(py)Ru^{IV}{=}O]^{2+},HO_2^- \xrightarrow[k_{IV,HO_2^-}]{} [b_2(py)Ru^{III}{-}O]^{+},HO_2 \quad (11)$$

$$[b_2(py)Ru^{III}{-}O]^{+},HO_2 \xrightarrow[\text{rapid}]{} [b_2(py)Ru^{III}{-}OH]^{2+} + O_2^-$$

$$[b_2(py)Ru^{III}{-}OH]^{2+} + O_2^- \xrightarrow[\text{rapid}]{} [b_2(py)Ru^{II}{-}OH]^{2+} + O_2$$

At 25 °C, K_a values for HO_2 and $[(bpy)_2(py)Ru^{II}(H_2O)]^{2+}$ are 4.69 ± 0.08 (I = 1.0 M)[32] and 10.20 (I = 0.1 M),[21,22,33] respectively.

Although there are other mechanisms available to $Ru^{IV}{=}O^{2+}$ for the oxidation of H_2O_2, they are either less likely or can be ruled out on the basis of the available experimental evidence.

(1) With coordinatively labile metal oxidants, direct evidence for inner-sphere oxidation following initial coordination of H_2O_2 has been found. There are no labile coordination sites in the $Ru^{IV}{=}O^{2+}$ oxidant.

(2) There is an extensive chemistry between H_2O_2 and metal or non-metal oxides involving the formation of peroxy acids

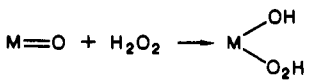

or cyclic peroxides

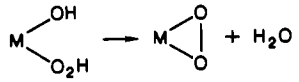

for low-coordinate, acidic metal oxides like CrO_3, WO_3, or V_2O_5.[34] The $Ru^{IV}{=}O^{2+}$ complex is somewhat crowded sterically,[1a] but neither peroxo

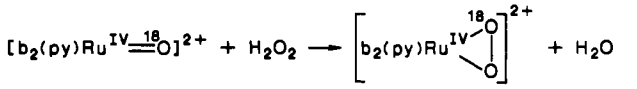

nor peroxy acid intermediates

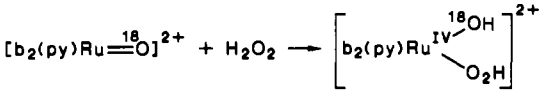

can be rejected out of hand. However, the ^{18}O labeling experiment would appear to rule out a peroxo intermediate given the appearance of ^{16}O–^{16}O as the product. A peroxy acid intermediate also seems unlikely based on the large k_{H_2O}/k_{D_2O} kinetic isotope effect and the slow rate of O exchange between the Ru^{IV}–oxo group and H_2O, which suggests that exchange pathways based on intermediates like

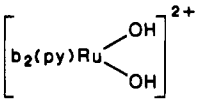

are slow.[22,35]

(3) O atom transfer appears to be a well-defined oxidative pathway for $Ru^{IV}{=}O^{2+}$ in its oxidations of PPh_3 to $OPPh_3$ and of sulfides to sulfoxides.[35,36] O atom transfer to H_2O_2 could occur via an intermediate dioxygen complex

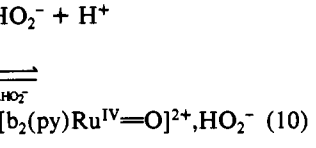

followed by displacement of bound O_2

$$[b_2(py)Ru^{II}{-}^{18}O{-}O]^{2+} + H_2O \rightarrow [b_2(py)Ru^{II}{-}OH_2]^{2+} + {}^{18}O{-}O$$

The ^{18}O labeling experiment rules out such a pathway in water. It can be ruled out in acetonitrile as well on the basis of the appearance of $[(bpy)_2(py)Ru^{II}(H_2O)]^{2+}$ as the initial product. If the dioxygen complex were an intermediate, the acetonitrile complex would have been the initially formed product via

$$[b_2(py)Ru^{II}{-}O{-}O]^{2+} + CH_3CN \rightarrow [b_2(py)Ru(CH_3CN)]^{2+} + O_2$$

Details of the H_2O_2 Oxidation Pathways. From the large k_{H_2O}/k_{D_2O} kinetic isotope effects and 1-equiv nature of the reactions, the oxidation of H_2O_2 by $[(bpy)_2(py)Ru^{IV}(O)]^{2+}$ or by $[(bpy)_2(py)Ru^{III}(OH)]^{2+}$ occurs by "H atom" or "proton-assisted electron transfer" in which synchronous proton and electron transfer occur between H_2O_2 and the complexes

$$[b_2(py)Ru^{IV}{=}O]^{2+},H_2O_2 \rightarrow [b_2(py)Ru{-}O{\cdots}H{\cdots}O_2H]^{2+} \rightarrow [b_2(py)Ru^{III}{-}OH]^{2+},O_2H \quad (12)$$

$$[b_2(py)Ru^{III}{-}OH]^{2+},H_2O_2 \rightarrow [b_2(py)Ru{-}O{\cdots}H{-}O_2H]^{2+} \rightarrow [b_2(py)Ru^{II}{-}OH_2]^{2+},O_2H \quad (13)$$

In the redox step the H^+/e-accepting roles of the oxidant are split with the metal acting as the electron acceptor and the oxo or hydroxo groups as the proton acceptor. Given the energetics of H atom formation from H_2O_2

$$[b_2(py)Ru^{IV}{=}O]^{2+},H_2O_2 \rightarrow [b_2(py)Ru^{IV}{=}O]^{2+},H,O_2H \qquad \Delta G^{\circ\prime} \sim 3.6 \text{ eV}$$

in no sense do the mechanisms involve actual formation of a discrete H atom that is in equilibration with its surroundings. Rather, a situation exists where in the interconversion between electronically weakly coupled reactants, e.g., $[(bpy)_2(py)Ru(O)]^{2+},H_2O_2$ and products, $[(bpy)_2(py)Ru(OH)]^{2+},O_2H$, strong, outer-sphere $\nu(H{-}O_2H)$ vibrationally induced electronic coupling must occur. The situation is different for an inner-sphere reaction involving initial binding, e.g., $M^{n+} + H_2O_2 \rightarrow M(H_2O_2)^{n+}$, where strong electronic coupling between the oxidant, M^{n+}, and reductant, H_2O_2, is induced by chemical bonding. In the H atom transfer case, strong electronic coupling is induced by the coupled H^+/e-transfer act itself.

Although a quantitative description of the H atom transfer pathway is not available, some comments can be made on the basis of the known properties of the reactants and the anticipated properties of the pathway: (1) The HOMO for H_2O_2 is a combination of σ(O—O) and an orbital of π^* symmetry.[37] For the Ru(IV)=O^{2+} complex there are two nearly degenerate d_π orbitals (t_{2g} in O_h symmetry) that are strongly mixed with p orbitals of the oxo group. Because of the π^* character in the HOMO of H_2O_2, a symmetry-allowed orbital basis exists for Ru(IV)=O^{2+}—H_2O_2 electronic coupling along the H—O_2H bond. (2) The preequilibria, K'_{IV,H_2O_2} in eq 6 and K'_{III,H_2O_2} in eq 8, are included in the experimentally measured rate constants and activation parameters since $k_{1,IV} = (K'_{IV,H_2O_2})(k_{IV,H_2O_2})$ and $k_{1,III} = (K'_{III,H_2O_2})(k_{III,H_2O_2})$. The preequilibria include contributions from preassociation of the reactants and a statistically based orientational factor arising from those few relative orientations of the reactants that allow H atom transfer to occur. (3) Although not tested here experimentally, in a H atom transfer there is no net

(32) Bielski, B. H. *Photochem. Photobiol.* **1978**, *28*, 645.
(33) Takeuchi, K. J.; Thompson, M. S.; Pipes, D. W.; Meyer, T. J. *Inorg. Chem.* **1984**, *23*, 1845–1850.
(34) Shelton, R. A.; Kochi, J. K. *Metal-Catalyzed Oxidations of Organic Compounds*; Academic: New York, 1981.
(35) Moyer, B. A.; Sipe, B. K.; Meyer, T. J. *Inorg. Chem.* **1981**, *20*, 1745.
(36) Roecker, L.; Dobson, J.; Meyer, T. J. *Inorg. Chem.*, in press.
(37) Back, R. D.; Wolber, G. J.; Coddeus, B. A. *J. Am. Chem. Soc.* **1984**, *106*, 6098.

charge transfer between reactants and it is expected that the redox steps in reactions 7 and 9 should be relatively solvent independent. (4) Significant contributions to the reaction must come from the normal modes of the reactants which are largely ν(Ru—O) and ν(H—O_2H) in character. A shift in ν(Ru—O) of > 500 cm^{-1} is expected in the conversion from Ru^{IV}=O^{2+} to Ru^{III}—OH^{2+}; $\nu(Ru^{IV}=O^{2+})$ = 790 cm^{-1}.[22] The large k_{H_2O}/k_{D_2O} kinetic isotope effects demonstrate the importance of ν(H—O_2H). Participation of this mode can best be viewed as involving "nuclear tunneling" from levels low in the potential curve, but any detailed calculation must include in an explicit way vibrationally induced electronic coupling. The fact that the isotope effect appears in both the $\Delta H^{\ddagger}$ ($\Delta H^{\ddagger}_{D_2O} - \Delta H^{\ddagger}_{H_2O}$ = 3.2 kcal/mole) and $\Delta S^{\ddagger}$ ($\Delta S^{\ddagger}_{D_2O} - \Delta S^{\ddagger}_{H_2O}$ = +2 eu) terms shows that because of the lower zero-point energy for ν(D—O_2H) there is advantage in the deuteriated case for thermal activation to levels above v = 0 where vibrational overlap is higher. Presumably, if the kinetic measurements could have been extended to lower temperature the expected temperature dependence of $\Delta H^{\ddagger}_{D_2O}$ would have been observed, ultimately with the low-temperature limit being reached. In the low-temperature limit all reactivity would be via v = 0 levels for both H_2O_2 and D_2O_2, $\Delta H^{\ddagger}_{D_2O} - \Delta H^{\ddagger}_{H_2O} \sim 0$, and the isotope effect is predicted to appear in $\Delta S^{\ddagger}$ because of lesser vibrational overlaps for D–O_2D given the lower zero-point energy. The low-temperature limit has been observed at 25 °C in the oxidation of benzyl alcohol by $[(bpy)_2(py)Ru^{IV}(O)]^{2+}$

$$[b_2(py)Ru^{IV}=O]^{2+} + PhCH_2OH \rightarrow [b_2(py)Ru^{II}—OH_2]^{2+} + PhCHO$$

where (k_{C-H}/k_{C-D}) = 50, $\Delta H^{\ddagger}_{C-D} - \Delta H^{\ddagger}_{C-H} \sim 0$, and the mechanism is thought to involve hydride transfer.[29]

The energetics of the H atom transfer step based on $E^{\circ\prime}$ = 0.76 V for the $[(bpy)_2(py)Ru^{IV}(O)]^{2+}/[(bpy)_2(py)Ru^{III}(OH)]^{2+}$ couple and $E^{\circ\prime}$ = 1.09 V for the H_2O_2/HO_2 couple at pH 7 vs. NHE[38] are illustrated in reaction 14. The overall reaction is spontaneous

$$[b_2(py)Ru^{IV}=O]^{2+},H_2O_2 \xrightarrow[E^{\circ\prime}= -0.30\ V]{} [b_2(py)Ru^{III}—OH]^{2+},HO_2 \quad (14)$$

by 0.49 V but the initial H atom step is nonspontaneous by −0.30 V because of the thermodynamic instability of HO_2. A considerable fraction of the free energy of activation of $\Delta G^{\ddagger}$(25 °C) = 16.5 kcal/mol has its origin solely in overcoming the uphill nature of the initial step (~7 kcal/mol), which is in addition to the vibrational demands imposed by the H atom transfer.

In the oxidation of H_2O_2 the H atom transfer pathway, although somewhat demanding mechanistically, is more facile than outer-sphere electron transfer where the mechanistic demands are minimal. The greater facility of the more complex pathway arises because both the Ru^{IV}=O^{2+}/Ru^{III}—OH and H_2O_2/HO_2 couples have proton demands that are not met by simple electron transfer. An initial outer-sphere electron transfer is highly unfavorable thermodynamically

$$[b_2(py)Ru^{IV}=O]^{2+},H_2O_2 \xrightarrow{k_{os}} [b_2(py)Ru^{III}—O]^{+},H_2O_2^{+} \quad (15)$$

For reaction 15, $E^{\circ\prime} \geq -1.06$ V, using $pK_a > 13$ for $[(bpy)_2(py)Ru^{III}(OH)]^{2+}$ and $pK_a < 0$ for $H_2O_2^{+}$. Using this value as the minimum free energy of activation for the outer-sphere electron-transfer pathway and a preexponential factor of $10^{13} \sim k_BT/h$ gives $k_{os} \leq 10^{13} \exp(-\Delta G^{\ddagger}/RT) \leq 3 \times 10^{-3}$ s^{-1}, which is considerably smaller than $k_{obsd} = (K'_{IV,H_2O_2})(k_{IV,H_2O_2})$ = 2.1 M^{-1} s^{-1} at 25 °C.

From the viewpoint of O_2 activation and the direct formation of H_2O_2, possibilities more interesting than H atom transfer are 2-electron hydride transfer

$$[b_2(py)Ru^{IV}=O]^{2+},H_2O_2 \rightarrow [b_2(py)Ru^{II}—OH]^{2+},O_2,H^{+}$$

and synchronous hydride–proton (two H atom) transfer

$$[b_2(py)Ru^{IV}=O]^{2+},H_2O_2 \rightarrow [b_2(py)Ru^{II}—OH_2]^{2+},O_2$$

The successful operation of either pathway in microscopic reverse would provide direct access to H_2O_2 from O_2. The inability of these pathways to compete in H_2O_2 oxidation may be a consequence at the molecular level of the difficulty of correlating the proton loss with the hydride transfer in the first case and the overall difficult structural demands imposed by the latter.

Acknowledgments are made to the National Institutes of Health under Grant No. 5-RO1-GM32296-03 for support of this research.

Registry No. $[(bpy)_2(py)Ru(O)]^{2+}$, 67202-43-1; $[(bpy)_2(py)Ru(OH)]^{2+}$, 75495-07-7; H_2O_2, 7722-84-1; D_2, 7782-39-0.

Supplementary Material Available: A table of rate constants for the oxidation of H_2O_2 by Ru^{IV}=O^{2+} and Ru^{III}—OH^{2+} at various temperatures (Table 1S) and figures illustrating an absorbance vs. time curve for the oxidation of H_2O_2 by Ru^{III}—OH^{2+} (Figure 1S) and showing plots of ln (k_{obsd}/T) vs. $1/T$ for the oxidations of H_2O_2 (Figure 2S) and D_2O_2 (Figure 3S) by Ru^{IV}=O^{2+} and the oxidation of H_2O_2 by Ru^{III}—OH^{2+} (Figure 4S) (7 pages). Ordering information is given on any current masthead page.

(38) Mulazzo, G.; Caroli, S. *Tables of Standard Electrode Potentials*; Wiley-Interscience: New York, 1978.